Specific Sequences in the N-terminal Domain of Human Small Heat Shock Protein HSPB6 Dictate Preferential Heterooligomerization with the Orthologue HSPB1

Michelle Heirbaut[1], Frederik Lermyte[2] , Esther M. Martin[2,3], Steven Beelen[1], Frank Sobott[2,3,4], Sergei V. Strelkov[1,5], Stephen D. Weeks[1,5]

[1] Laboratory for Biocrystallography, Dept. of Pharmaceutical and Pharmacological Sciences, KU Leuven, Belgium
[2] Biomolecular and Analytical Mass Spectrometry Group, Dept. of Chemistry, University of Antwerp, Belgium
[3] Astbury Centre for Structural Molecular Biology, University of Leeds, Leeds LS2 9JT, United Kingdom
[4] School of Molecular and Cellular Biology, University of Leeds, LS2 9JT, United Kingdom

Running title: N-terminal determinants of HSPB6 heterooliogomerization

[5] To whom correspondence should be addressed:
Sergei V. Strelkov, Laboratory for Biocrystallography, Department of Pharmaceutical and Pharmacological Sciences, Herestraat 49 box 822, B-3000 Leuven, Belgium, Tel: +32 16330845, Fax: +32 16323469, e-mail: sergei.strelkov@kuleuven.be,
Stephen D. Weeks, Laboratory for Biocrystallography, Department of Pharmaceutical and Pharmacological Sciences, Herestraat 49 box 822, B-3000 Leuven, Belgium, Tel: +32 16377204, Fax: +32 16323469, e-mail: stephen.weeks@kuleuven.be

Keywords: chaperone, cysteine-mediated cross-linking, mass spectrometry (MS), site-directed mutagenesis, small heat shock protein (sHSP), protein-protein interaction, protein complex, small-angle X-ray scattering (SAXS), Hsp20, Hsp27

ABSTRACT

Small heat shock proteins (sHSPs) are a conserved group of molecular chaperones with important roles in cellular proteostasis. Although sHSPs are characterized by their small monomeric weight, they typically assemble into large polydisperse oligomers that vary in both size and shape but are principally composed of dimeric building blocks. These assemblies can comprise different sHSP orthologues, creating additional complexity that may affect chaperone activity. However, the structural and functional properties of such heterooligomers are poorly understood. We became interested in heterooligomer formation between human heat shock protein family B (small) member 1 (HSPB1) and HSPB6, which are both highly expressed in skeletal muscle. When mixed in vitro, these two sHSPs form a polydisperse oligomer array composed solely of heterodimers, suggesting preferential association that is determined at the monomer level. Previously, we have shown that the sHSP N-terminal domains (NTDs), which have a high degree of intrinsic disorder, are essential for the biased formation. Here we employed iterative deletion mapping to elucidate how the NTD of HSPB6 influences its preferential association with HSPB1 and show that this region has multiple roles in this process. First, the highly conserved motif RLFDQxFG is necessary for subunit exchange among oligomers. Second, a site approximately 20 residues downstream of this motif determines the size of the resultant heterooligomers. Third, a region unique to HSPB6 dictates the preferential formation of heterodimers. In conclusion, the disordered NTD of HSPB6 helps regulate the size and stability of heterooligomeric complexes, indicating that terminal sHSP regions define the assembly properties of these proteins.

Heat shock proteins are an indispensable group of proteins in charge of maintaining cellular proteostasis. This protein superfamily ensures both

the correct folding of newly synthesized proteins and prevents unfolding and aggregation under stress conditions (1). Small heat shock proteins (sHSPs) are an important subfamily of this network and capture proteins in the early stages of unfolding, thereby preventing aberrant interactions leading to aggregation (2). sHSPs are capable of binding a wide variety of substrate proteins within the cell, and are considered a first line of defense of the protein quality control network (3–6).

Small heat shock proteins are notorious for assembling into large polydisperse complexes, comprised of up to 40 subunits for some members (7–9). These assemblies are formed from dimeric building blocks, where the constituent monomeric subunits can freely exchange (10). Dimer association is mediated by the core structured region of sHSPs, the α-crystallin domain (ACD) (11–14). Crystal structures of the isolated ACD of a number of metazoan sHSPs show a 7-stranded β-sandwich that readily assembles into dimers via anti-parallel pairing of the β7-strand (15–17). Within this kingdom higher order assembly into the larger oligomeric species, as well as regulation of subunit exchange of the component protomers, is controlled via the N- and C-terminal arms that flank the ACD (18). Other than the presence of a tripeptide IxI/V motif, termed the C-terminal anchoring module (19), these domains are generally considered to be poorly conserved and are predicted to lack secondary structure making characterization of their role in assembly particularly challenging.

This multifaceted structural association and dynamics is further complicated by heterooligomerization, in which two or more orthologous sHSPs co-assemble into the typical high molecular weight complexes (20–24). This phenomenon has been described for bacterial, plant and metazoan sHSPs (21, 25, 26). In humans, numerous members of the sHSP family have been shown to interact with each other (23), the most well-known complex being lens α-crystallin, which is composed of αA- and αB-crystallin in a 3:1 monomer ratio (27, 28). Although present in this ratio in most vertebrate lenses, when mixed in vitro they form a hetero-oligomer containing subunits consistent with the proportion used (29, 30). The α-crystallin heterocomplex therefore shows a ratio of the component sHSPs that likely reflects their relative expression levels. At the same time, there are number of human orthologues that, when mixed together in various ratios, form heterooligomers with a specific subunit stoichiometry (20, 31).

In this study we focus on the biologically relevant complex formed between HSPB1 and HSPB6, two sHSPs that coassemble in muscle tissue where they are both highly expressed (32, 33). Previous studies of the human HSPB1 and HSPB6 heterooligomers have shown that they form highly polydisperse complexes containing an equimolar amount of each sHSP (31, 34). Assuming both sHSPs can freely exchange subunits, random protomer turnover would be expected to result in oligomers containing both homo and heterodimers. Recently, using native mass spectrometry, we have observed that although both sHSPs alone can exchange subunits in such a stochastic fashion, the heterooligomeric complex is composed solely of heterodimers (35). This result, in good agreement with earlier residue specific cross-linking studies (21), supports a heterooligomer model where HSPB1 and HSPB6 preferentially associate at the core dimer level. Curiously this preferred association, which is mediated by the ACD, requires the presence of the highly flexible NTDs (35). This latter region of human HSPB1 is 90 residues long and has low sequence homology with the 72 residue NTD of HSPB6, with the most prominent exception being a conserved RLFDQxFG motif close to the center of this domain in the two proteins. Due to these distinct differences, how this disordered region dictates the association properties of the structured ACD is not understood.

Here we have used a library of deletion constructs, previously employed to investigate the role of the NTD of HSPB6 in chaperoning (36), to identify the N-terminal residues in this sHSP that dictate heterooligomerization. The effect of these deletions, as well additional point mutants, on the subunit exchange behavior with HSPB1 were analyzed by an array of techniques including size exclusion chromatography, mass spectrometry (MS) and disulfide mediated cross-linking studies. The results point to a complex mechanism where different sequences within the NTD of HSPB6 influence the initial association of the two sHSPs, the size of the resultant heterooligomeric assemblies, and the preferential heterodimerisation with HSPB1.

RESULTS

Deletion mapping of the HSPB6 NTD defines regions involved in heterooligomersation

N-terminal deletion constructs of human HSPB6, used previously to identify substrate binding sites of this sHSP (36), were employed to map the residues within the NTD that are required for the preferential association with HSPB1. Previous characterization of these HSPB6 constructs showed that they were all dimeric in solution, similar to the wild type (WT) protein. This thus permits an investigation of the possible effect of truncation on the size distribution of formed heterooligomers without fear of interference of aberrant homooligomers of the deletion constructs.

The equimolar mixture of WT HSPB1 and HSPB6 prepared at 37^{o}C yielded a broad elution profile on analytical SEC, composed of two peaks with maxima corresponding to a molecular weight of 508 and 160 kDa, in line with previous studies (35). The corresponding eluted fractions contained equimolar amounts of both sHSPs when analysed by SDS-PAGE (Fig. 1). All seven HSPB6 deletion constructs were capable of forming a heterooligomer with HSPB1, albeit with differing elution profiles for some (Fig. 1). Most notably, deletion of residues 51-60 led to the predominant formation of the smaller heterooligomeric species at the expense of the larger complex, despite these entities containing equal amounts of both sHSPs in SDS-PAGE analysis of the fractions. Another striking difference was observed with constructs that lack residues 21-30 and 31-40. In both cases not all of the HSPB6 construct was incorporated into the complex, as evidenced by a dominance of HSPB1 in the SDS-PAGE analysis of fractions of the heterooligomer peak, as well as by a small remnant peak of the HSPB6 deletant alone in the SEC chromatogram (Fig. 1).

SEC-coupled SAXS experiments of the same mixtures showed a single elution peak, likely due to a lower resolving power of the Shodex column compared to the Superdex 200 column (Supplemental Fig. 1). The calculated average mass of the complex between both WT proteins corresponds to 360 kDa and has a R_g value of 51 Å at the elution peak maxima, with a range of 39.5 to 52.4 Å (Table 1). This is smaller than the WT HSPB1 but larger than WT HSPB6, which have a R_g at the elution peak of 58 Å and 32 Å respectively. Combined these values are in agreement with the heterooligomer being a polydisperse mixture containing species whose size ranges vary between those of the component homooligomers (Fig. 1, Supplemental Fig. 1). For the majority of complexes formed between the different HSPB6 deletions and HSPB1, the peak R_g value as well as the R_g range were similar to that of the WT complex. However, the deletion of residues 51-60 resulted in a clearly smaller species with a peak R_g of 41.6 Å. At the same time, the two truncations that did not form a complex with HSPB1 efficiently (Δ21-30 and Δ31-40) showed an increased peak R_g value of 57 Å as well as a wider range in R_g from 57 Å to 33 Å. This correlates well with the higher resolution SEC studies that showed the presence of both a larger species, containing predominantly HSPB1, as well the non-associated HSPB6 deletion dimeric species (Fig. 1).

To ascertain whether the heterooligomers formed between HSPB1 and the different HSPB6 truncations were composed primarily of heterodimers, disulfide cross-linking was used. To this end, an additional double mutation C46S.E116C (denoted by an asterisk in subsequent construct names) was introduced in every HSPB6 deletion construct. A single mutation E116C was introduced in Δ41-50 where the native cysteine is absent. E116 and the corresponding residue C137 in HSPB1 residue in the β7 strand of the ACD are located near the two-fold axis of the AP_{II} dimer interface (Fig. 2A, Supplemental Fig. 3A) (16, 18). This proximal position of the cysteines means that both WT HSPB1 and the HSPB6* mutant can be readily cross-linked across the dimer interface by oxidation (16). Likewise, disulfide cross-linking of the heated HSPB1/HSPB6* mixture yields a species with a mass between that of the HSPB1 and HSPB6 cross-linked dimers when analyzed by non-reducing SDS-PAGE (Fig. 2B and C). Importantly introduction of the C46S.E116C double mutation results in wild type exchange behavior (21). In our hands the additionally mutated HSPB6 truncations all behaved like their non-mutant equivalent during purification (data not shown).

The results of the disulfide cross-linking clearly show that all HSPB6 truncations except for Δ21-30* and Δ31-40* are nearly fully engaged in

a heterodimeric complex with HSPB1, just like the full-length proteins (Fig. 2B). In contrast, the Δ21-30* and Δ31-40* constructs, when incubated with HSPB1, reveal three bands, corresponding to cross-linked HSPB1 homodimer, the heterodimer and the HSPB6* homodimers respectively. As assessed by densitometry of the stained gels, the molar ratio of these species was close to 1:0.5:1 (corresponding to 20% heterodimer formation). This suggests that the deletion of these regions in HSPB6 hampers the heterodimer formation. To test whether the Δ21-30* and Δ31-40* constructs were capable of forming a cross-dimer disulfide when alone, a control oxidation experiment was performed that demonstrated that they oxidized as readily as all other constructs under the conditions employed (Fig. 2C). To rule out the further possibility that the Δ21-30 and Δ31-40 deletions limited HSPB6 subunit exchange, native MS analysis of ^{15}N-labeled sample mixed in a 1:1 ratio with non-labeled sample was performed. The MS spectra showed that in both cases subunit turnover was not limited, as a stochastic 1:2:1 ratio of non-labeled, monolabeled and dilabeled dimers was observed (Supplemental Fig. 2).

In addition, native MS experiments with the preincubated 1:1 mixtures of HSPB1 and the various HSPB6 truncations were performed (Fig. 3). Just like the WT protein, all HSPB6 truncations except for Δ21-30 and Δ31-40, revealed almost exclusively the presence of hetero-dimers with HSPB1. The lack of detection of larger heterooligomeric species was previously observed, and likely due to both the low protein concentrations used and less efficient detection of the resulting high-m/z ions (35). Experiments involving the Δ11-20, Δ41-50 and Δ51-60 constructs additionally showed a small fraction of HSPB6 homodimers, and dissociated monomers, which could be due to a slight molar excess of the HSPB6 construct due to inaccuracies in concentration determination. Crucially for the Δ21-30 and Δ31-40 HSPB6 constructs no heterodimer was observed (HSPB1 is not visible in these spectra, as it occurs as larger oligomers – mainly tetramer – under these conditions). Thus both the cysteine cross-linking and the native MS experiments together suggest that the region found between residues 21 to 40 of HSPB6 is necessary for heterocomplex formation with HSPB1.

Specific contributions of several regions within the HSPB6 NTD in heterocomplex assembly

To investigate the regions that influence heterooligomerization in more detail, a series of HSPB6 constructs with shorter deletions were cloned and purified. First of all, we evaluated which amino acids in the region encompassing residues 51-60 are responsible for the formation of the larger heterooligomeric species (which are diminished upon deletion of this sequence, Fig. 1) by creating two 5aa deletion constructs. Analytical SEC analysis of HSPB1 preincubated with the HSPB6 Δ56-60 construct showed a profile exactly like that of the mixture of the WT sHSPs, whereas deletion of residues 51-55 biased the hetero-oligomer profile to the smaller species (Fig. 4A). Residues within this latter region are found to be somewhat conserved in other HSPB6 homologues known to interact with this sHSP, the core of which is a tripeptide sequence where the terminal residues are typically proline and tyrosine (Fig. 4B) (26).

Next, we addressed the contribution of the HSPB6 region encompassing residues 21-40. The results from SEC and disulfide cross-linking on the four 5aa HSPB6 deletions (Fig. 5) provided more detail on the involvement of this region in heterooligomer formation. The Δ26-30, Δ31-35 and Δ36-40 constructs demonstrated a SEC profile (Fig. 5A) similar to that obtained for the Δ21-30 and Δ31-40 deletions (Fig. 1). In particular all featured the presence of a more-or-less resolved peak containing only HSPB6 homodimers. At the same time, the Δ21-25 construct behaved like the WT protein (Fig. 5A). As before, the C46S.E116C double mutation was introduced into each truncation to examine heterodimer formation by disulfide cross-linking (Fig. 5B). As expected the Δ21-25* construct showed wild type behavior, revealing almost exclusively cross-linked heterodimers with HSPB1 on a non-reducing SDS-PAGE. In contrast, the remaining three 5aa deletion constructs revealed the presence of both homo- and heterodimers, with some specific differences between them. In the case of Δ26-30* and Δ31-35*, densitometry of the various disulfide-linked species showed approximately 20% heterodimer formation. This suggests that these two 5aa deletions are severely limited in their ability to form hetero-oligomers with

HSPB1, similar to the corresponding 10aa deletions (Fig. 2B and 5B). At the same time, these two smaller deletion constructs fully oxidize on their own (Fig. 5C). For Δ36-40*, the bands corresponding to HSPB1 homodimers, heterodimers and HSPB6 homodimers had a molar ratio of 1:2:1, suggesting a stochastic exchange of monomers. For each of the 5aa deletions, the ratios of the two homodimers and the heterodimer seen on a non-reducing SDS-PAGE could be further confirmed by analyzing the cross-linked samples using MS under denaturing conditions (Fig. 5E).

As the disulfide cross-link is chemically labile and can exchange with non-oxidised species, we confirmed the observed differences between the four constructs using the chemical cross-linker bismaleimidoethane (BMOE; Supplemental Fig. 3). One of the preferred configurations of this compound results in the maleimide groups being at a suitable distance to cross-link the cysteine residues at the dimer interface. Incubation of the preheated mixtures with BMOE for only 15 mins at 4°C resulted in a pattern that was equivalent to that seen by disulfide mediated cross-linking (Fig. 5B and Supplemental Fig. 3C).

The differences between the Δ26-30/Δ31-35 constructs and the Δ36-40 construct point to a possible dual role played by the central part of the HSPB6 NTD. Firstly, residues 26 to 35, which contain the highly conserved RLFDQxFG motif (Fig. 5D), are necessary for facilitating subunit exchange. Secondly the residues 36 to 40 appear to define the preferential heterodimeric interaction between both sHSPs.

Asymmetric roles of equivalent NTD regions in HSPB1 and HSPB6

Since residues 27 to 34 within the NTD of HSPB6 are highly conserved in HSPB1 (Fig. 5D), we wondered whether homologous deletions in HSPB1 would have a similar effect on the heterooligomer formation. To this end, we created the HSPB1.Δ26-30 and HSPB1.Δ31-35 constructs each being an equivalent of the corresponding 5aa deletant of HSPB6 (the residue numbering is consistent between the two proteins in this region). Both HSPB1 truncations readily formed heterooligomeric complexes with WT HSPB6 as observed by SEC (Fig. 6A and B), while disulfide cross-linking experiments revealed that such complexes were predominantly built from heterodimers (Fig. 6C). These results are in strong contrast with the observations for the equivalent deletions in HSPB6, which had a negative effect on subunit exchange between the two orthologues (Fig. 5).

Curiously the HSPB1.Δ26-30 construct readily formed heterooligomers with HSPB6 at 4°C, yielding a SEC profile that was only seen for the WT sHSP mixture when heated to 37°C (Fig. 6A). This observation can possibly be attributed to an increase in HSPB1 subunit turnover, thereby allowing interaction with HSPB6 even at low temperatures. It should be noted that HSPB1.Δ26-30 alone forms somewhat smaller oligomers than the WT HSPB1, evident from a shift of the SEC elution peak during purification (data not shown). In addition, HSPB1.Δ26-30 does not cross-link efficiently with itself (Fig. 6C), a result that suggests that residues 26-30 may be important for HSPB1 oligomerization, or might somehow affect the register of the ACD dimer interface (16). When incubated at 37°C, the heterooligomers formed by HSPB1.Δ26-30 and HSPB6 showed a major peak at 300 kDa, a value that is an intermediate of the two peaks usually observed for the WT HSPB1 and HSPB6 hetero-oligomers (Fig. 6A). In comparison, heterooligomerisation of the HSPB1.Δ31-35 construct and HSPB6 occurred only upon incubation at 37°C, and led to the formation of heterooligomeric complexes which revealed an asymmetric SEC profile with a single maximum at 500 kDa, corresponding to the larger heterooligomer species seen when mixing both WT proteins (Fig. 6A).

The results from deletion of the 26-35 region in HSPB1 suggest there is an asymmetry between HSPB1 and HSPB6 in the role of this highly conserved sequence for heterooligomer formation. To assess whether this depends on the small sequence differences in this region between the two sHSPs, or is driven in part by their context within the respective full-length proteins, two domain swaps of this region were created (Fig. 7A). These 10-residue swaps change the sequence **G**RLFDQ**R**FG**E** of HSPB6 to **S**RLFDQ**A**FG**L** of HSPB1 and vice versa, which corresponds to triple mutantions indicated in bold. Swapping of these residues led to wild type heterooligomerisation behavior for HSPB6 containing the HSPB1

sequence (HSPB6.10swap) when mixed with WT HSPB1. The opposite swap in HSPB1 (HSPB1.10swap) also yielded heterooligomers, but with a preference for forming predominantly larger assemblies (Fig. 7B). In both cases, the complexes readily oxidized when mixing with the appropriate HSPB6* mutant yielding mainly heterodimers when analyzed by non-reducing SDS-PAGE showing that the mutations did not hamper heterodimersation (Fig. 7C).

An equimolar mixture of the two 10swap mutants resulted in a SEC profile similar to that seen with the HSPB1.10swap and WT HSPB6 (Fig. 7B). The asymmetric elution, with a single maximum at ~500 kDa, was also observed with the HSPB1.Δ31-35 construct (Fig. 6B) and points to a role of either A32 or L35 of HSPB1 in the concentration-dependent formation of the second smaller heterooligomeric species typically observed with the mixtures of the WT proteins (Fig 7B). The fact that the mixture of the two 10swap mutants did not result in a wild type SEC profile, despite the HSPB6 chimera containing the HSPB1 26-35 region, suggests that the mode of action of A32 or L35 occurs only when they found within the full-length HSPB1 protein.

To investigate the role of residues 36-40 in driving preferential heterodimerization, we also swapped this region between the two sHSPs (Fig. 7A). These swaps correspond to four mutations in each construct, exchanging residues **GLLEA** of HSPB6 to **PR**L**PE** of HSPB1 (HSPB6.5swap) and vice versa (HSPB1.5swap). When mixed with HSPB1 the HSPB6.5swap chimera led to only stochastic subunit exchange as observed by SEC and cross-linking studies using the HSPB6.5swap* mutant (Fig. 7B and C). This behavior was equivalent to that seen with the HSPB6.Δ36-40 deletion construct and points to the role of one or more of the mutated residues in heterodimer formation. The converse HSPB1.5swap with HSPB6 resulted in heterodimer formation, albeit yielding heterooligomers of a much higher molecular weight than seen with the WT proteins (Fig. 7B and C). The fact that the HSPB1.5swap, which is effectively HSPB6-like in the 36-40 region, did not demonstrate stochastic exchange with HSPB6 as has been reported for the latter sHSP alone (35), suggests that the preferential heterodimerization between these two sHSP is not driven by these positionally equivalent regions interacting with each other in the heterooligomer. Combined these results support a model where residues 36-40 in HSPB6 likely interact with different residues in HSPB1 to drive the formation of the heterodimer. The asymmetric behavior of this region in both sHSPs was further evaluated by mixing the two 5swap constructs together. The presence of remnant HSPB6 in the SEC profile suggests that residues 36-40 only acts within the context of the surrounding NTD residues in HSPB6 (Fig. 7B).

Mapping of specific residues involved in heterooligomerization

The slight bias in overall heterooligomer size for the HSPB1.10swap was further investigated by point mutations. Since most of the sequence is similar, we decided to mutate the differing residues in the conserved stretch. HSPB6 has an arginine at position 32 where HSPB1 has an alanine (Fig. 5D). A point mutation was created in both sHSPs to convert it to the sequence of the other and these confirmed the results seen using the larger swaps: HSPB1.A32R (B6-like) form complexes with HSPB6 that are larger than with the WT HSPB1, whereas HSPB6.R32A (B1-like) demonstrates a SEC profile that is wild type (Fig. 8A). When mixing both mutations, the same profile was seen as for the HSPB1.A32R-HSPB6 complex, showing that this arginine is acting within the context of HSPB1 and is responsible for the larger size oligomers, whereas this residue in HSPB6 does not seem to be involved in interactions (results not shown).

As neither of the 10swap constructs mimicked the behavior seen for the Δ26-30 and Δ31-35 constructs of HSPB6, point mutations of the key conserved residues were also created. It has been shown previously that phenylalanines in the NTD play an important role in intersubunit contacts (37). This region in HSPB1 and HSPB6 contains two such residues. We therefore generated mutants of one (F33A) or both (F29A and F33A, termed FFAA) for each sHSP. Different permutations of these mutants, mixed with either the WT or mutant partner, were examined. Mixing HSPB6.F33A with WT HSPB1 led to a chromatogram similar to that obtained for HSPB6.Δ31-35 (Fig. 8A), suggesting that this phenylalanine residue in HSPB6 is important in

heterooligomer formation, a result confirmed by disulfide cross-linking using the HSPB6.F33A* mutant (Fig. 8B). However, the opposite experiment, mixing WT HSPB6 with HSPB1.F33A, did not hamper the preferred heterodimerisation of these two sHSPs as evaluated by the oxidation experiment (Fig. 8B). Unexpectedly though, the HSPB1.F33A mutation led to exchange of subunits at 4°C, as evidenced by a reduction of the HSPB6 peak, and the formation of smaller heterooligomeric species (~300 kDa) following heating. This behavior was similar to that observed with the HSPB1.Δ26-30 deletion mutant (Figs. 8A and 6A). As seen before, this suggests an asymmetric role for this highly conserved residue in defining the interaction between these two sHSPs.

When mixing the HSPB1.F33A and HSPB6.F33A, together a unique chromatogram was observed (Fig. 8A). The broad profile at 4°C showed two peaks overlapping, suggesting some mixing of the two mutants at low temperature. After incubation at 37°C, a shift in the ratio of the peak maximas could be noticed but the overall shape of the elution profile remained similar to the unheated sample. Disulfide cross-linking showed a minor fraction of heterodimers as similar to that seen for the mixture of WT HSPB1 and HSPB6.F33A* (Fig. 8B). Combined, the data suggests that these mutants can associate at lower temperatures but subunit exchange is severely hampered.

The results for the double mutations (FFAA) looked exactly like those for the single phenylalanine substitutions, alluding to a more important role for F33 than F29 in both proteins (Fig. 8A). It should be noted that the mutations in HSPB1 yielded smaller homooligomers than the WT protein as assessed by SEC during purification (results not shown), and that the FFAA construct did not cross-link to the same extent as the WT protein on its own (Fig. 8C). This suggests an important role for the phenylalanine residues in HSPB1 homooligomerization. These phenyl-alanines thus seem essential to allow the interaction between HSPB1 and HSPB6 and are involved in important intersubunit contacts in the oligomeric assemblies.

DISCUSSION

Heterooligomerization of sHSPs has long been recognized in different organisms, although the exact function and benefit of such assemblies is still unknown. As many members of the family tend to form such mixed oligomers, information about their structure and the determinants of the assembly process should help to understand the chaperone activity of sHSPs and their interaction with different partner proteins. We have focused our attention on HSPB1 and HSPB6, two human sHSPs that are highly expressed in muscle tissue (33).

Previously it has been shown that HSPB1 and HSPB6 preferentially form heterooligomers over interactions with other orthologues (21). This is most likely the result of their propensity to yield species composed solely of heterodimers when mixed together (35), suggesting a biased association at the level considered to be the basic building block of the larger oligomeric assemblies. Surprisingly, deletion constructs of the two proteins corresponding to the ACD - the only structured region that form the core dimer interface (15–17) - were found to heterooligomerize in a stochastic fashion (35). It is the NTD, a region shown to be largely unstructured in HSPB6 and predicted to have similar properties in HSPB1 (18), that is essential for this preferred association. Employing a comprehensive set of deletion mutants of HSPB6 we have identified three regions of importance within its NTD that affect the heterooligomer assembly with HSPB1 (Table 2).

Firstly, we have discovered that a conserved motif P(G/F/Y)Y, which is located at position 52-54 in the second half of the NTD of HSPB6 and found at an equivalent position in a number of other orthologues known to interact with this sHSP (Fig. 4B), seems to regulate the size of the resultant heterooligomer. Deletion of these residues in HSPB6 leads to the formation of smaller heterooligomeric species with HSPB1, albeit composed of the canonical heterodimers (Fig. 9). Predictions suggest that this region in both proteins, like the majority of the NTD, contain no secondary structural elements (Supplemental Fig. 4). This is in good agreement with a recent X-ray crystallographic structure of the full-length HSPB6 bound to a 14-3-3 adapter protein which showed that this part of the NTD is highly disordered (38). However, studies of

HSPB5 oligomers, using solid-state NMR, report that the homologous region in this sHSP shows chemical shifts resembling a β-strand (39). Therefore it is possible that in the higher-order assemblies formed between HSPB1 and HSPB6 some structure is induced that is necessary for association. Indeed the importance of this region in HSPB5 has been highlighted by pin array experiments, where peptides encompassing this sequence were identified to interact with HSPB4 (40), suggesting a possible conserved role in hetero-association.

Secondly, we have found that the highly conserved RLFDQxFG sequence (36), is a prerequisite of heterooligomerization. Intriguingly this motif is always present in sHSPs reported to form heterooligomers with HSPB6 (Fig. 5D), but is absent in a number of homologues, including HSPB3 (Supplemental Fig, 4C), an sHSP that has been shown not to interact with HSPB6 (20). This predicted unstructured sequence (Fig. 5D) appears to be necessary for the exchange of HSPB6 subunits with HSPB1. This region was previously identified as a negative regulator of activity in HSPB6 and was also found to control both size and activity in αB-crystallin (36, 41). Specifically our results point to the highly conserved phenylalanines F29 and F33 as essential for the HSPB1/HSPB6 association. Despite their conservation between the two sHSPs, there appears to be an asymmetry in their importance. Just like the deletion of residues 31-35, mutation of F33 in HSPB6 effectively blocked hetero-association, whereas mutation of the equivalent residue in HSPB1 led to the formation of smaller oligomers but still composed of heterodimers. The involvement of phenylalanines of the NTD in controlling sHSP association and size has also been observed in the fission yeast SpHSP16.0 where the mutation of F6 or F7 led to an impairment of oligomer formation (37). The residue bias of phenylalanines in the NTD in genome-wide studies suggests this is likely a common phenomenon (42).

Thirdly, we have identified a region in the NTD of HSPB6, with no functional equivalent in HSPB1, which is responsible for the preferential heterodimerization of these two sHSPs. Specifically deletion or mutation of residues 36-40 of HSPB6 resulted in a protein that could form heterooligomers with HSPB1, but contained HSPB1 and HSPB6 homodimers alongside the heterodimers. Importantly the observed molar ratio of the three species suggest a stochastic exchange of subunits at the monomer level. The same behavior was seen for the heterooligomerization of HSPB1 and HSPB6 truncations each missing the whole NTD (35). Since swapping of this sequence into HSPB1 had no observable effect on subunit exchange, that is that the HSPB1.5swap chimera did not show a preferred association with itself over HSPB6, we conclude that these residues function within the context of the heterodimer. Thus the 36-40 region is somehow responsible for stabilizing the interface of the ACDs occurring within a heterodimer. The aforementionedstructure of HSPB6 in complex with a 14-3-3 adapter protein has shown that regions of the NTD can thread through the shared groove formed between the β3-strands of the ACD dimer (38). Patching of this same groove in the heterodimer, by one of more residues in the 36-40 region of HSPB6, could possibly stabilize this new interface and explain the asymmetric behavior of this interaction.

A recent study of heterooligomer formation between HSPB5 and HSPB6 has proposed a model in which the C-terminal IxI/V-motif of HSPB5 is required for the initial capture of the HSPB6 dimer, whereupon a new heterodimer interface is formed and stabilized by the NTD of HSPB6 (43). Assuming a similar model of association between HSPB1 and HSPB6 the results presented here can extend our understanding of this association further (Fig. 9). Initially, HSPB6 is recruited to the HSPB1 homooligomer via the interaction of its ACD with the C-terminal IxI/V-motif of HSPB1. Although an equivalent C-terminal localized motif is missing in HSPB6, its ACD has been shown to readily bind sequences containing this tripeptide sequence (18, 38, 43, 44). Following this capture step incorporation of HSPB6 into the HSPB1 oligomer is dependent, firstly, on the formation of HSPB1/HSPB6 heterodimers. Indeed, Mymrikov et al. (21) have shown that heterooligomerization is blocked by disulfide cross-linking of both sHSPs prior to mixing. Therefore stable incorporation of HSPB6 is dependent on localized dissociation of both the HSPB1 and HSPB6 homodimers and subunit exchange, in agreement with the earlier model (43). Secondly our data

shows the conserved NTD motif, and in particular residue F33, plays an important role in this initial subunit exchange. In the case of HSPB1, mutation of this residue to alanine enhances the recruitment of HSPB6, while the equivalent mutation in HSPB6 severely hampers this process. This suggests that the conserved motif of HSPB6 must displace an interaction made by the same sequence in the HSPB1 homooligomers to permit homodimer dissociation and subunit exchange (Fig. 9). Finally, our experiments show that, uniquely for the HSPB1 and HSPB6 mixed complex, residues 36-40 of the latter sHSP enhances preferential hetero-association at the ACD interface in the heterooligomers. Whether this HSPB6 mediated biased association already occurs during initial subunit incorporation, or appears as a result of the free exchange of subunits in the heterooligomeric species as presented in Fig. 9, cannot be ascertained from the equilibrium experiments performed here.

The involvement of the NTD in defining the strength and specificity of the newly formed ACD dimer interface is quite remarkable. Indeed, we have found this intrinsically disordered region to be highly implicated in dictating the properties of the sole structured region in these proteins. Similar involvement of the NTD and CTD have been published for HSPB5, where binding of the CTD destabilizes the dimer interface (45), and phosphorylation of N-terminal serine residues leads to loss of dimeric substructure in the homooligomers (46). In summary, modifications such as phosphorylation within the NTD may have a profound effect on the structure of sHSPs and can even lead to a destabilization of the ACD dimer interface, suggesting that indeed this region must interact with the ACD core and function either as a stabilizer or destabilizer, dependent on the modifications present.

Many reviews have acknowledged the potential of sHSPs both as drug targets and for biotechnological applications (47–51). To create inhibitors or enhancers of sHSP activity, a detailed understanding of their function and the sequences involved is necessary. Similarly, to use sHSPs as nanomaterials for activities such as targeted drug delivery or imaging purposes, it is crucial that we understand the sequence properties that define the size and shape of these oligomers. Studies focusing on sHSP heterooligomerization could bring us one step closer to eventually designing sHSPs with tailored properties.

This work is the first to fully explore the sequence properties in defining hetero-oligomerization of two human sHSPs. The results described here show a complicated yet important interplay between the NTD, which features a high degree of intrinsic disorder, and the structured ACD, in regulating size and stability of the complexes, proving that the terminal regions in sHSPs play an important role in defining their assembly properties. As these same regions also have a role in chaperone activity (35, 36), a correlation between the ability to heterooligomerize and to protect substrates from aggregating should be logically expected. A systematic investigation of this interplay, which is clearly relevant in vivo, is necessary.

EXPERIMENTAL PROCEDURES

Mutagenesis and cloning - The previously described small ubiquitin modifier (SUMO)-fusions of HSPB1 and HSPB6 (16) were used as a template for the generation of additional deletion constructs and point mutations. Point mutations were created using site-directed mutagenesis. DpnI-treated PCR products were transformed into E. coli NEB5α (New England Biolabs) and positive clones were verified by sequencing. A double mutant C46S.E116C of HSPB6, in which the native cysteine-46 is mutated to serine, and glutamate-116 at the dyad axis of the ACD dimer is mutated to cysteine, was created using two rounds of mutagenic PCR. This mutant was also used as a template to create additional N-terminal deletions using a PCR-based overlap mutagenesis method described previously (36). A similar approach was employed to generate the HSPB1 and HSPB6 sequence swaps. All constructs were designed such that, upon cleavage of the linearly fused SUMO chimera with recombinant SUMO-hydrolase, no additional non-native residues were present on the target protein (52).

Expression and purification - All constructs were transformed into the E. coli Rosetta 2 (DE3) pLysS strain (Novagen) and clones were cultured in ZYP-5052 auto-inducing medium (53) using described conditions (16). Cell were harvested by centrifugation at 8000 x g, resuspended in buffer (50 mM sodium phosphate,

250 mM sodium chloride and 12.5 mM imidazole, pH7.5) and stored at -80°C. For the expression of ^{15}N-labeled proteins, transformed clones were cultured in 2 mL of LB medium for 7h. This culture was then transferred to 50 mL of P0.5G-medium (53) and grown overnight at 25°C. 10 mL of this culture was spun down at 3000 rcf and the pellet was transferred to 200 mL of auto-inducing minimal medium containing ^{15}N-ammonium chloride (53). Cells were grown and harvested using the same conditions as above.

Cells were thawed and diluted in the same buffer complemented with 1 unit/mL of Cryonase Cold Active Nuclease (Clontech) and 10 mM $MgCl_2$. Cells were lysed by sonication in 3 cycles with 20 minutes in between each cycle. Further purification by IMAC, ion exchange and size exclusion was performed as described previously (36, 52). ^{15}N-labeled proteins were purified using the same protocol except the final SEC was performed using a Superdex 200 10/300 GL column pre-equilibrated in 200 mM ammonium acetate pH6.9 containing 2.5 mM DTT.

Analytical size-exclusion chromatography - Prior to analysis, 220 µM (corresponding to 5 mg/ml for HSPB1) of each protein was mixed in 20 mM HEPES pH 7.4, 150 mM NaCl and 10mM DTT to produce hetero-oligomeric complexes. The mix was incubated overnight at 37°C to allow complete subunit exchange. 100 µL of each protein or complex was loaded onto a Superdex 200 10/300 GL column (GE Healthcare Life Sciences), pre-equilibrated at 4°C in 20 mM HEPES pH 7.2, 150 mM NaCl and 2.5 mM DTT using a flow-rate of 0.5 mL/min. The column was calibrated using standards from the Molecular Weight Calibration kit (GE Healthcare Life Sciences) including blue dextran, ferritin, aldolase, conalbumin, ovalbumin, carbonic anhydrase, ribonuclease A and aprotinin. The standards were diluted in the same buffer and run under the same conditions.

Disulfide cross-linking - For oxidation cross-linking experiments, 50 µM of each protein was mixed in 50 mM sodium phosphate pH 7.5, 100 mM NaCl and 5 mM DTT, incubated overnight at 37°C, and then subjected to dialysis for 48 hr at 20°C with the same buffer without DTT. 10 µL from this mixture was analyzed on a non-reducing SDS-PAGE containing 15% acrylamide. Reduced controls were obtained by diluting the samples with buffer with DTT before loading. Densitometry using ImageJ of the Coomassie-stained gels was used to quantify the molar amounts of protein present in each band, whereby the reference bands containing the known molar amounts of fully oxidized HSPB6*, HSPB1 or the HSPB6*/HSPB1 heterodimers were used for calibration.

Chemical cross-linking – The purified proteins were dilaysed against 50 mM sodium phosphate, 100 mM NaCl, 1 mM EDTA, and 2 mM Tris(2-carboxyethyl)phosphine (TCEP), pH 7.5 at 4°C. The buffer was exchanged three times to ensure the complete removal of DTT. A solution containing 50 µM of each construct (i.e. 100 µM total sHSP for the 1:1 mixtures of HSPB1 and each HSPB6* mutant) was prepared and heated at 42°C for 1.5 hr. TCEP was then removed from each reaction using a Zeba spin desalting column with a 40 kDa molecular weight cutoff (ThermoFisher Scientific) pre-equilibrated with 50 mM sodium phosphate, 100 mM NaCl, 1 mM EDTA pH 7.5. The samples, containing no reducing agent, were split in half and placed at 4°C. To one tube a 1.1 molar excess of bismaleimidoethane (BMOE), solubilized in DMSO, was added. Following a 15 min incubation period 10 µL of each reaction was taken and cross-linking stopped by the addition of SDS-PAGE loading buffer containing 100 mM β-mercaptoethanol. The second tube, containing no cross-linker, was incubated for 1 hr at 4°C. At this point a 10 µL sample was taken and diluted in SDS-PAGE sample buffer containing no reducing agent. All samples were analyzed by SDS-PAGE using a 12-15% acrylamide gradient.

Mass spectrometry - All MS measurements were performed on a quadrupole/ion mobility/time-of-flight instrument with ion mobility capabilities (Synapt G2 HDMS, Waters, Wilmslow, UK), operated in positive ion mode. Data acquisition and processing were performed using MassLynx (version 4.1) and external calibration up to 5000 m/z was performed with CsI solution.

For native MS analyses of the complexes, 200 µM (monomer concentration) of each protein was mixed together in 200 mM ammonium acetate pH 6.9, 2.5 mM DTT and incubated overnight at 37°C. The samples were further dialyzed against the same buffer in three exchanges, over a 24 hr

period, to ensure complete removal of nonvolatile salt. Approximately 5 µL of solution containing 20 µM of protein (monomer concentration) diluted with the 200 mM ammonium acetate pH 6.9, 2.5 mM DTT buffer was transferred to gold-coated glass capillaries prepared in-house and infused into the mass spectrometer using the nanoflow version of the Z-spray ion source. A capillary voltage of 1.0 – 1.3 kV and minimal (<0.2 bar) nanoflow gas pressure were used, and the instrument was operated in Mobility/Sensitivity mode. Instrument parameters were as follows unless stated otherwise: sample cone 80 V, extraction cone 1 V, backing pressure 3.2 – 4.5 mbar, source pressure 4.6e-3 – 5.8e-3 mbar, trap collision energy 10 V, trap DC bias 50 V, transfer collision energy 5 V. The IM cell was filled with 3.5 mbar of N_2 (He cell gas flow 180 mL/min, IMS gas flow 60 mL/min), and IM wave height and velocity were 40 V and 1000 m/s, respectively.

MS analyses of cross-linked species were performed in the denatured state on the same instrument, but in this case the protein concentration was reduced to 2 µM (monomer concentration) in 50 % acetonitrile and 1% formic acid. The instrument was operated in TOF/Sensitivity mode for these experiments, with the following settings: capillary voltage 1.0 kV, sampling cone 40 V, extraction cone 2 V, backing pressure 2.5 mbar, source pressure 4.1e-3 mbar, trap collision energy 4 V, trap DC bias 5 V, transfer collision energy 0 V. Spectra were subsequently deconvoluted using the MaxEnt 1 module of the MassLynx software to determine relative abundances.

Small-angle X-ray scattering - The measurements were performed at Synchrotron Soleil (Saint-Aubin, France) as described previously (36). 80 µL sample containing 5 mg/ml HSPB1 (equivalent to approximately 220 µM) and the molar equivalent of HSPB6, incubated at 45°C for 1 h to form complexes, which has been shown to be sufficient for complex formation (31), was loaded onto a Shodex KW-404F column at 0.2 ml/min pre-equilibrated with 50 mM sodium phosphate pH 7.5, 100 mM NaCl and 2.5 mM DTT. During each run, 100 frames were recorded prior to the start of the protein elution towards evaluating the buffer scattering. Thereafter 250 frames were recorded while the complex eluted from the column. The exposure time per frame was 750 ms, with a dead time of 1500 ms between frames. Data processing was done as described previously (35).

Acknowledgments: This research was supported by the Research Foundation Flanders (FWO) grants G093615N and WO03315N as well as by the KU Leuven grant OT13/097 (all to S.V.S.). M.H. has held a teaching assistant grant from the Department of Pharmaceutical and Pharmacological Sciences, KU Leuven. We also thank the FWO for funding a PhD fellowship of F.L. (grant no. 11L4115N) and the Hercules Foundation Flanders for funding the Synapt instrument. We acknowledge support from the European Community's Seventh Framework Programme under the BioStruct-X initiative (project number 6131) towards the synchrotron SAXS measurements. The authors further greatly appreciate the excellent support from the beamline scientists on the SWING beamline (Soleil Synchrotron, France).

Conflict of interest: The authors declare that there is no conflict of interest

Author contributions: MH and SDW conceived and designed the experiments. MH, FL, EMM, SB and SDW contributed various reagents, performed experiments and analyzed the data. MH, FL, FS, SVS and SDW were involved in data interpretation and preparation of the manuscript. All authors reviewed the results and approved the final version of the manuscript.

REFERENCES

1. Kim, Y. E., Hipp, M. S., Bracher, A., Hayer-Hartl, M., and Ulrich Hartl, F. (2013) Molecular Chaperone Functions in Protein Folding and Proteostasis. Annual Review of Biochemistry. **82**, 323–355
2. Haslbeck, M., and Vierling, E. (2015) A First Line of Stress Defense: Small Heat Shock Proteins and Their Function in Protein Homeostasis. J. Mol. Biol. **427**, 1537–1548
3. Haslbeck, M. (2002) sHsps and their role in the chaperone network. Cell. Mol. Life Sci. **59**, 1649–1657
4. Basha, E., Lee, G. J., Breci, L. A., Hausrath, A. C., Buan, N. R., Giese, K. C., and Vierling, E. (2004) The identity of proteins associated with a small heat shock protein during heat stress in vivo indicates that these chaperones protect a wide range of cellular functions. J. Biol. Chem. **279**, 7566–7575
5. Andley, U. P., Malone, J. P., and Townsend, R. R. (2014) In Vivo Substrates of the Lens Molecular Chaperones αA-Crystallin and αB-Crystallin. PLoS ONE. **9**, e95507
6. Mymrikov, E. V., Daake, M., Richter, B., Haslbeck, M., and Buchner, J. (2017) The Chaperone Activity and Substrate Spectrum of Human Small Heat Shock Proteins. J. Biol. Chem. **292**, 672–684
7. Clauwaert, J., Ellerton, H. D., Koretz, J. F., Thomson, K., and Augusteyn, R. C. (1989) The effect of temperature on the renaturation of alpha-crystallin. Curr. Eye Res. **8**, 397–403
8. Baldwin, A. J., Lioe, H., Hilton, G. R., Baker, L. A., Rubinstein, J. L., Kay, L. E., and Benesch, J. L. P. (2011) The polydispersity of αB-crystallin is rationalized by an interconverting polyhedral architecture. Structure. **19**, 1855–1863
9. Lermyte, F., Williams, J. P., Brown, J. M., Martin, E. M., and Sobott, F. (2015) Extensive Charge Reduction and Dissociation of Intact Protein Complexes Following Electron Transfer on a Quadrupole-Ion Mobility-Time-of-Flight MS. J. Am. Soc. Mass Spectrom. **26**, 1068–1076
10. Haslbeck, M., Franzmann, T., Weinfurtner, D., and Buchner, J. (2005) Some like it hot: the structure and function of small heat-shock proteins. Nat Struct Mol Biol. **12**, 842–846
11. Haley, D. A., Horwitz, J., and Stewart, P. L. (1998) The small heat-shock protein, alphaB-crystallin, has a variable quaternary structure. J Mol Biol. **277**, 27–35
12. Aquilina, J. A., Benesch, J. L. P., Bateman, O. A., Slingsby, C., and Robinson, C. V. (2003) Polydispersity of a mammalian chaperone: mass spectrometry reveals the population of oligomers in alphaB-crystallin. Proc. Natl. Acad. Sci. U.S.A. **100**, 10611–10616
13. Mymrikov, E. V., Seit-Nebi, A. S., and Gusev, N. B. (2011) Large potentials of small heat shock proteins. Physiol. Rev. **91**, 1123–1159
14. Basha, E., O'Neill, H., and Vierling, E. (2012) Small heat shock proteins and α-crystallins: dynamic proteins with flexible functions. Trends Biochem. Sci. **37**, 106–117
15. Bagnéris, C., Bateman, O. A., Naylor, C. E., Cronin, N., Boelens, W. C., Keep, N. H., and Slingsby, C. (2009) Crystal Structures of α-Crystallin Domain Dimers of αB-Crystallin and Hsp20. J. Mol. Biol. **392**, 1242–1252
16. Baranova, E. V., Weeks, S. D., Beelen, S., Bukach, O. V., Gusev, N. B., and Strelkov, S. V. (2011) Three-Dimensional Structure of α-Crystallin Domain Dimers of Two Human Small Heat Shock Proteins, HSPB1 and HSPB6. J. Mol. Biol. **411**, 110–122
17. Hochberg, G. K. A., Ecroyd, H., Liu, C., Cox, D., Cascio, D., Sawaya, M. R., Collier, M. P., Stroud, J., Carver, J. A., Baldwin, A. J., Robinson, C. V., Eisenberg, D. S., Benesch, J. L. P., and Laganowsky, A. (2014) The structured core domain of αB-crystallin can prevent

amyloid fibrillation and associated toxicity. Proc. Natl. Acad. Sci. U.S.A. **111**, E1562-1570
18. Weeks, S. D., Baranova, E. V., Heirbaut, M., Beelen, S., Shkumatov, A. V., Gusev, N. B., and Strelkov, S. V. (2014) Molecular structure and dynamics of the dimeric human small heat shock protein HSPB6. J. Struct. Biol. **185**, 342–354
19. Poulain, P., Gelly, J.-C., and Flatters, D. (2010) Detection and architecture of small heat shock protein monomers. PLoS ONE. **5**, e9990
20. Engelsman, J. den, Boros, S., Dankers, P. Y. W., Kamps, B., Vree Egberts, W. T., Böde, C. S., Lane, L. A., Aquilina, J. A., Benesch, J. L. P., Robinson, C. V., de Jong, W. W., and Boelens, W. C. (2009) The small heat-shock proteins HSPB2 and HSPB3 form well-defined heterooligomers in a unique 3 to 1 subunit ratio. J Mol Biol. **393**, 1022–1032
21. Mymrikov, E. V., Seit-Nebi, A. S., and Gusev, N. B. (2012) Heterooligomeric complexes of human small heat shock proteins. Cell Stress Chaperones. **17**, 157–169
22. Aquilina, J. A., Shrestha, S., Morris, A. M., and Ecroyd, H. (2013) Structural and functional aspects of hetero-oligomers formed by the small heat shock proteins αB-crystallin and HSP27. J. Biol. Chem. **288**, 13602–13609
23. Arrigo, A.-P. (2013) Human small heat shock proteins: Protein interactomes of homo- and hetero-oligomeric complexes: An update. FEBS Lett. **587**, 1959–1969
24. Sobott, F., Benesch, J. L. P., Vierling, E., and Robinson, C. V. (2002) Subunit exchange of multimeric protein complexes. Real-time monitoring of subunit exchange between small heat shock proteins by using electrospray mass spectrometry. J. Biol. Chem. **277**, 38921–38929
25. Studer, S., and Narberhaus, F. (2000) Chaperone activity and homo- and hetero-oligomer formation of bacterial small heat shock proteins. J. Biol. Chem. **275**, 37212–37218
26. Basha, E., Jones, C., Wysocki, V., and Vierling, E. (2010) Mechanistic differences between two conserved classes of small heat shock proteins found in the plant cytosol. J. Biol. Chem. **285**, 11489–11497
27. Spector, A., Li, L. K., Augusteyn, R. C., Schneider, A., and Freund, T. (1971) -Crystallin. The isolation and characterization of distinct macromolecular fractions. Biochem. J. **124**, 337–343
28. Augusteyn, R. C. (2004) alpha-crystallin: a review of its structure and function. Clin Exp Optom. **87**, 356–366
29. Srinivas, P. N. B. S., Reddy, P. Y., and Reddy, G. B. (2008) Significance of alpha-crystallin heteropolymer with a 3:1 alphaA/alphaB ratio: chaperone-like activity, structure and hydrophobicity. Biochem. J. **414**, 453–460
30. Sun, T. X., and Liang, J. J. (1998) Intermolecular exchange and stabilization of recombinant human alphaA- and alphaB-crystallin. J. Biol. Chem. **273**, 286–290
31. Bukach, O. V., Glukhova, A. E., Seit-Nebi, A. S., and Gusev, N. B. (2009) Heterooligomeric complexes formed by human small heat shock proteins HspB1 (Hsp27) and HspB6 (Hsp20). Biochim Biophys Acta. **1794**, 486–495
32. Kato, K., Goto, S., Inaguma, Y., Hasegawa, K., Morishita, R., and Asano, T. (1994) Purification and characterization of a 20-kDa protein that is highly homologous to alpha B crystallin. J. Biol. Chem. **269**, 15302–15309
33. Sugiyama, Y., Suzuki, A., Kishikawa, M., Akutsu, R., Hirose, T., Waye, M. M., Tsui, S. K., Yoshida, S., and Ohno, S. (2000) Muscle develops a specific form of small heat shock protein complex composed of MKBP/HSPB2 and HSPB3 during myogenic differentiation. J. Biol. Chem. **275**, 1095–1104

34. Bukach, O. V., Seit-Nebi, A. S., Marston, S. B., and Gusev, N. B. (2004) Some properties of human small heat shock protein Hsp20 (HspB6). Eur. J. Biochem. **271**, 291–302
35. Heirbaut, M., Lermyte, F., Martin, E. M., Beelen, S., Verschueren, T., Sobott, F., Strelkov, S. V., and Weeks, S. D. (2016) The preferential heterodimerization of human small heat shock proteins HSPB1 and HSPB6 is dictated by the N-terminal domain. Arch. Biochem. Biophys. **610**, 41–50
36. Heirbaut, M., Beelen, S., Strelkov, S. V., and Weeks, S. D. (2014) Dissecting the Functional Role of the N-Terminal Domain of the Human Small Heat Shock Protein HSPB6. PLoS ONE. **9**, e105892
37. Hanazono, Y., Takeda, K., Oka, T., Abe, T., Tomonari, T., Akiyama, N., Aikawa, Y., Yohda, M., and Miki, K. (2013) Nonequivalence observed for the 16-meric structure of a small heat shock protein, SpHsp16.0, from Schizosaccharomyces pombe. Structure. **21**, 220–228
38. Sluchanko, N. N., Beelen, S., Kulikova, A. A., Weeks, S. D., Antson, A. A., Gusev, N. B., and Strelkov, S. V. (2017) Structural Basis for the Interaction of a Human Small Heat Shock Protein with the 14-3-3 Universal Signaling Regulator. Structure. **25**, 305–316
39. Jehle, S., Vollmar, B. S., Bardiaux, B., Dove, K. K., Rajagopal, P., Gonen, T., Oschkinat, H., and Klevit, R. E. (2011) N-terminal domain of alphaB-crystallin provides a conformational switch for multimerization and structural heterogeneity. Proc. Natl. Acad. Sci. U.S.A. **108**, 6409–6414
40. Ghosh, J. G., and Clark, J. I. (2005) Insights into the domains required for dimerization and assembly of human alphaB crystallin. Protein Sci. **14**, 684–695
41. Pasta, S. Y., Raman, B., Ramakrishna, T., and Rao, C. M. (2003) Role of the conserved SRLFDQFFG region of alpha-crystallin, a small heat shock protein. Effect on oligomeric size, subunit exchange, and chaperone-like activity. J. Biol. Chem. **278**, 51159–51166
42. Heirbaut, M., Strelkov, S. V., and Weeks, S. D. (2015) Everything but the ACD, Functional Conservation of the Non-conserved Terminal Regions in sHSPs. in The Big Book on Small Heat Shock Proteins (Tanguay, R. M., and Hightower, L. E. eds), pp. 197–227, Heat Shock Proteins, Springer International Publishing, **8**, 197–227
43. Delbecq, S. P., Rosenbaum, J. C., and Klevit, R. E. (2015) A Mechanism of Subunit Recruitment in Human Small Heat Shock Protein Oligomers. Biochemistry. **54**, 4276–4284
44. Delbecq, S. P., Jehle, S., and Klevit, R. (2012) Binding determinants of the small heat shock protein, αB-crystallin: recognition of the "IxI" motif. EMBO J. **31**, 4587–4594
45. Hilton, G. R., Hochberg, G. K. A., Laganowsky, A., McGinnigle, S. I., Baldwin, A. J., and Benesch, J. L. P. (2013) C-terminal interactions mediate the quaternary dynamics of αB-crystallin. Philos. Trans. R. Soc. Lond., B, Biol. Sci. **368**, 20110405
46. Aquilina, J. A., Benesch, J. L. P., Ding, L. L., Yaron, O., Horwitz, J., and Robinson, C. V. (2004) Phosphorylation of alphaB-crystallin alters chaperone function through loss of dimeric substructure. J. Biol. Chem. **279**, 28675–28680
47. James, M., Crabbe, C., and Hepburne-Scott, H. W. (2001) Small heat shock proteins (sHSPs) as potential drug targets. Curr Pharm Biotechnol. **2**, 77–111
48. Sun, Y., and MacRae, T. H. (2005) The small heat shock proteins and their role in human disease. FEBS J. **272**, 2613–2627
49. Flenniken, M. L., Uchida, M., Liepold, L. O., Kang, S., Young, M. J., and Douglas, T. (2009) A library of protein cage architectures as nanomaterials. Curr Top Microbiol Immunol. **327**, 71–93
50. Lin, Y., MaHam, A., Tang, Z., Wu, H., and Wang, J. (2009) Protein-Based Nanomedicine

Platforms for Drug Delivery. Small. **5**, 1706–1721
51. Furnish, E. J., Brophy, C. M., Harris, V. A., Macomson, S., Winger, J., Head, G. A., and Shaver, E. G. (2010) Treatment with transducible phosphopeptide analogues of the small heat shock-related protein, HSP20, after experimental subarachnoid hemorrhage: prevention and reversal of delayed decreases in cerebral perfusion. J Neurosurg. **112**, 631–639
52. Weeks, S. D., Drinker, M., and Loll, P. J. (2007) Ligation independent cloning vectors for expression of SUMO fusions. Protein Expr. Purif. **53**, 40–50
53. Studier, F. W. (2005) Protein production by auto-induction in high density shaking cultures. Protein Expr. Purif. **41**, 207–234
54. Kurowski, M. A., and Bujnicki, J. M. (2003) GeneSilico protein structure prediction meta-server. Nucleic Acids Res. **31**, 3305–3307
55. Ren, J., Wen, L., Gao, X., Jin, C., Xue, Y., and Yao, X. (2009) DOG 1.0: illustrator of protein domain structures. Cell Res. **19**, 271–273
56. Konarev, P. V., Volkov, V. V., Sokolova, A. V., Koch, M. H. J., and Svergun, D. I. (2003) PRIMUS : a Windows PC-based system for small-angle scattering data analysis. J. Appl. Crystallogr. **36**, 1277–1282
57. Petoukhov, M. V., Konarev, P. V., Kikhney, A. G., and Svergun, D. I. (2007) ATSAS 2.1 – towards automated and web-supported small-angle scattering data analysis. J. Appl. Crystallogr. **40**, s223–s228
58. Petoukhov, M. V., Franke, D., Shkumatov, A. V., Tria, G., Kikhney, A. G., Gajda, M., Gorba, C., Mertens, H. D. T., Konarev, P. V., and Svergun, D. I. (2012) New developments in the ATSAS program package for small-angle scattering data analysis. J. Appl. Crystallogr. **45**, 342–350

FOOTNOTES

The abbreviations used are: ACD, α-crystallin domain; CTD, C-terminal domain; MS, mass spectrometry; NTD, N-terminal domain; SAXS, small-angle X-ray scattering; SEC, size exclusion chromatography; sHSP, small heat shock protein.

FIGURE LEGENDS

FIGURE 1. Role of the NTD of HSPB6 in heterooligomerization. Analytical SEC profiles of equimolar mixtures of HSPB1 and each HSPB6 deletion following overnight incubation at 37°C. A 100 µl sample was loaded onto a Superdex 200 10/300 column equilibrated in 20 mM HEPES, 150 mM NaCl and 2.5 mM DTT. The chromatogram of the control sample (the equimolar mixture stored at 4°C) is shown as a grey filled curve, the heated mixture is shown as a black curve. Fractions (F) are denoted at the base of each curve, their identities are shown on the bottom left panel. Right-hand side, corresponding SDS-PAGE analysis of the fractions from analytical SEC. An input sample (i) of the equimolar mix of both sHSPS taken prior to injection onto the column, and the same sample diluted 10-fold (i/10) were also loaded.

FIGURE 2. Disulfide cross-linking studies of HSBP1/HSPB6* heterocomplexes. (A) Cartoon representation of the putative ACD heterodimer interface. Residues E116 of HSPB6 (green ribbons) and C146 of HSPB1 (cyan ribbons) are shown in red as all-atom representations. (B) Reducing SDS-PAGE analysis of HSPB1 and HSPB6 C46S.E116C (HSPB6*) constructs. (C) Non-reducing SDS-PAGE analysis of the complexes between HSPB1 and the seven different HSPB6* deletion constructs. Samples were incubated at 37°C overnight in 50 mM sodium phosphate pH 7.5, 100 mM NaCl and 5 mM DTT and then dialyzed against the same buffer without DTT to permit disulfide cross-linking. (D) Control experiment showing the non-reducing SDS-PAGE analysis of each HSPB6* deletion construct following extensive dialysis to remove DTT.

FIGURE 3. Native mass spectrometry analysis of mixtures of HSPB1 and the HSPB6 deletions. Native MS of the HSPB1-HSPB6 deletion complexes, 20 µM (monomer concentration) of each preincubated mixture in 200 mM ammonium acetate pH6.9 containing 2.5mM DTT was analyzed on a Synapt G2 HDMS (Waters). Charge states are indicated above each peak.

FIGURE 4. Iterative mapping of the region containing residues 51 to 60. (A) Analytical SEC profile of an equimolar mixture of HSPB1 and the HSPB6 Δ51-55 and Δ 56-50 truncations following overnight incubation at 37°C. The SEC profile of the control sample (mixture stored at 4°C) is shown as a black dashed line, the heterooligomer (incubated at 37°C) is shown as a continuous black line. For each chromatogram the profile of the heterooligomer for WT HSPB1 and HSPB6 is shown as a red dashed line. (B) Alignment of the 50-60 region of HSPB6 with equivalent sequences from human homologues reported to interact with this sHSP. Residues are highlighted using the Clustal color scheme. The numbering above the alignment corresponds to the residue position in human HSPB6. Uniprot accession numbers: HSPB6, O14558; HSPB1, P04792 ; HSPB2, Q16082; HSPB5, P02511; HSPB8; Q9UJY1.

FIGURE 5. Iterative mapping of residues 21 to 40 containing the conserved region. (A) Analytical SEC profiles of an equimolar mixture of HSPB1 with either HSPB6 Δ21-25, Δ26-30, Δ31-35 or Δ36-40 following overnight incubation at 37°C. The control sample (kept at 4°C) is shown with black dashed line, the hetero-oligomer (incubated at 37°C) is shown as a black line. For each chromatogram the hetero-oligomer for WT HSPB1 and HSPB6 is shown as a red dashed line. (B) Non-reducing SDS-PAGE analysis of the disulfide cross-linked complexes between HSPB1 and the four HSPB6* truncations. (C) Control experiment showing the non-reducing SDS-PAGE analysis of all oxidized constructs on their own. (D) Sequence alignment, and corresponding consensus secondary structure (CSS) predictions of the

21-40 region of HSPB6 and known interacting homologues. Aligned residues are shaded using the Clustal colour scheme. The numbering above the alignment corresponds to the residue position in human HSPB6. The database identity of each sequence is presented in the legend to Fig. 4. The CSS for each sequence was determined using the GeneSilico meta-server (54). (E) MaxEnt 1 deconvoluted mass spectra of oxidized samples.

FIGURE 6. Deletion of the conserved region in HSPB1. (A) Analytical SEC profiles of an equimolar mixture of HSPB1 Δ26-30 or Δ31-35 deletion constructs and WT HSPB6 following overnight incubation at 37°C. The control sample (sample kept at 4°C) is shown with black dashed lines, the hetero-oligomer (incubated at 37°C) is shown as a black line. For each chromatogram the hetero-oligomer for WT HSPB1 and HSPB6 is shown as a red dashed line. (B) Non-reducing SDS-PAGE analysis of the complexes between the HSPB1 deletions and HSPB6*. (C) Control experiment showing the non-reducing SDS-PAGE analysis of HSPB1 Δ26-30 or Δ31-35 following extensive dialysis to remove DTT.

FIGURE 7. Domain swapping of conserved region in HSPB1 and HSPB6. (A) Cartoon representation of the constructs used. The figures were created using DOG (55). (B) Analytical SEC profiles of an equimolar mixture of the various HSPB1 and HSPB6 swaps following overnight incubation at 37°C. The control sample (stored at 4°C) is shown as a black dashed line, the hetero-oligomer (incubated at 37°C) is shown as a continuous black line. For each chromatogram the hetero-oligomer for WT HSPB1 and HSPB6 is shown as a red dashed line. (C) Non-reducing SDS-PAGE analysis of the complexes between the HSPB1 and HSPB6* swaps. (C) Control experiment showing the non-reducing SDS-PAGE analysis of different constructs following extensive dialysis to remove DTT

FIGURE 8. Point mutation analysis of the conserved region in HSPB1 and HSPB6. (A) Analytical SEC profile of an equimolar mixture of various HSPB1 and HSPB6 point mutations following overnight incubation at 37°C. The control sample (stored at 4°C) is shown as a black dashed line, the hetero-oligomer (incubated at 37°C) is shown as continuous black line. For each chromatogram the hetero-oligomer for WT HSPB1 and HSPB6 is shown as a red dashed line. (B) Non-reducing SDS-PAGE analysis of the complex between HSPB1 and HSPB6* point mutants (C) Control experiment showing the non-reducing SDS-PAGE analysis of different constructs following extensive dialysis to remove DTT.

FIGURE 9. Cartoon summarizing the regions of HSPB6 involved in heterooligomer formation. (1) The CTD of HSPB1 recruits HSPB6 via patching of the hydrophobic groove formed between the β4 and β8-strands of the ACD (represented by semi-circle) of the latter sHSP. This interaction is blocked by mutation of S134 in HSPB6 and by disulfide cross-linking (S-S) of both proteins (21, 43). (2) Residue F33 of the NTD of HSPB6 destabilises the NTD interactions in the HSPB1 homooligomer permitting subunit exchange and full incorporation of HSPB6. (3) Within the resultant heterocomplex the individual subunits can freely exchange, (4) preferential heterodimerisation within the mixed oligomer is driven by residues 36-40 of HSPB6. (5) The heterooligomer is found in an equilibrium of two species, the populations of which are regulated by residues 51-55 in HSPB6.

TABLE 1. SAXS analysis of the hetero-oligomeric complexes of HSPB1 and HSPB6 deletion constructs. The SAXS frames were processed using AUTORG (56) and GNOM (56, 57). The second last column shows the R_g value at the elution peak. The last column shows the R_g range corresponding to the frames for which the quality measure in AUTORG was 50 % or higher.

Protein	Estimated average MW (kDa) based on Porod volume	Calculated average number of subunits	Peak R_g (Å)	R_g range
B1.WT	647.6	28.4	58.2	63.0 – 56.0
B6.WT	45.9	2.7	32.4	32.9 – 27.5
B1 + B6	342.4	17.2	51.1	52.4 – 39.5
B1 + B6.ΔN11	311.7	16.1	49.6	50.9 – 39.7
B1 + B6.Δ11-20	212.1	10.9	48.0	51.1 – 35.2
B1 + B6.Δ21-30	490.8	25.2	56.9	57.1 – 31.5
B1 + B6.Δ31-40	478.9	24.7	57.0	57.3 – 33.2
B1 + B6.Δ41-50	356.4	18.3	52.2	52.9 – 44.9
B1 + B6.Δ51-60	134.7	6.9	41.6	48.2 – 33.7
B1 + B6.Δ61-70	337.6	17.3	51.2	51.8 – 42.5

Table 2. Summary of the heterooligomerisation properties of HSPB6 deletions and point mutations with HSPB1.

10 amino acid deletions			5 amino acid deletions			Point mutations		
Construct	SEC[a]	S-S[b]	Construct	SEC[a]	S-S[b]	Construct[c]	SEC[a]	S-S[b]
ΔN11	WT	1	Δ21-25	WT	1	10swap	WT	1
Δ11-20	WT	1	Δ26-30	Remnant HSPB6	1:0.5:1	5swap	Remnant HSPB6	1:0.5:1
Δ21-30	Remnant HSPB6	1:0.5:1	Δ31-35	Remnant HSPB6	1:0.5:1	R32A	WT	1
Δ31-40	Remnant HSPB6	1:0.5:1	Δ36-40	Remnant HSPB6	1:2:1	F33A	Remnant HSPB6	1:0.5:1
Δ41-50	WT	1	Δ51-55	Small	1	FFAA	Remnant HSPB6	1:0.5:1
Δ51-60	Small	1	Δ56-60	WT	1			
Δ61-70	WT	1						

[a] SEC profile of each HSPB6 construct when mixed in equimolar amounts with HSPB1 and heated. 'WT': closely resembling the mixture of WT HSPB6 and HSPB1. 'Remnant HSPB6': chromatograms contain an additional late eluting peak corresponding to the HSPB6 dimer position. 'Small': chromatograms show a profile biased to an approximately 140kDa species.

[b] Ratio of disulfide crosslinked HSPB1 homodimer, HSPB1 and HSPB6 construct heterodimer, and HSPB6 construct homodimer as evaluated by non-reducing SDS-PAGE. A single value corresponds to heterodimers only.

[c] 10swap corresponds to the HSPB6 G26S\R32A\E35L mutant. The 5swap corresponds to the HSPB6 G36P\RL37R\E39P\A40E mutant. FFAA corresponds to the HSPB6 F29A\F33A mutant.

Figure 1

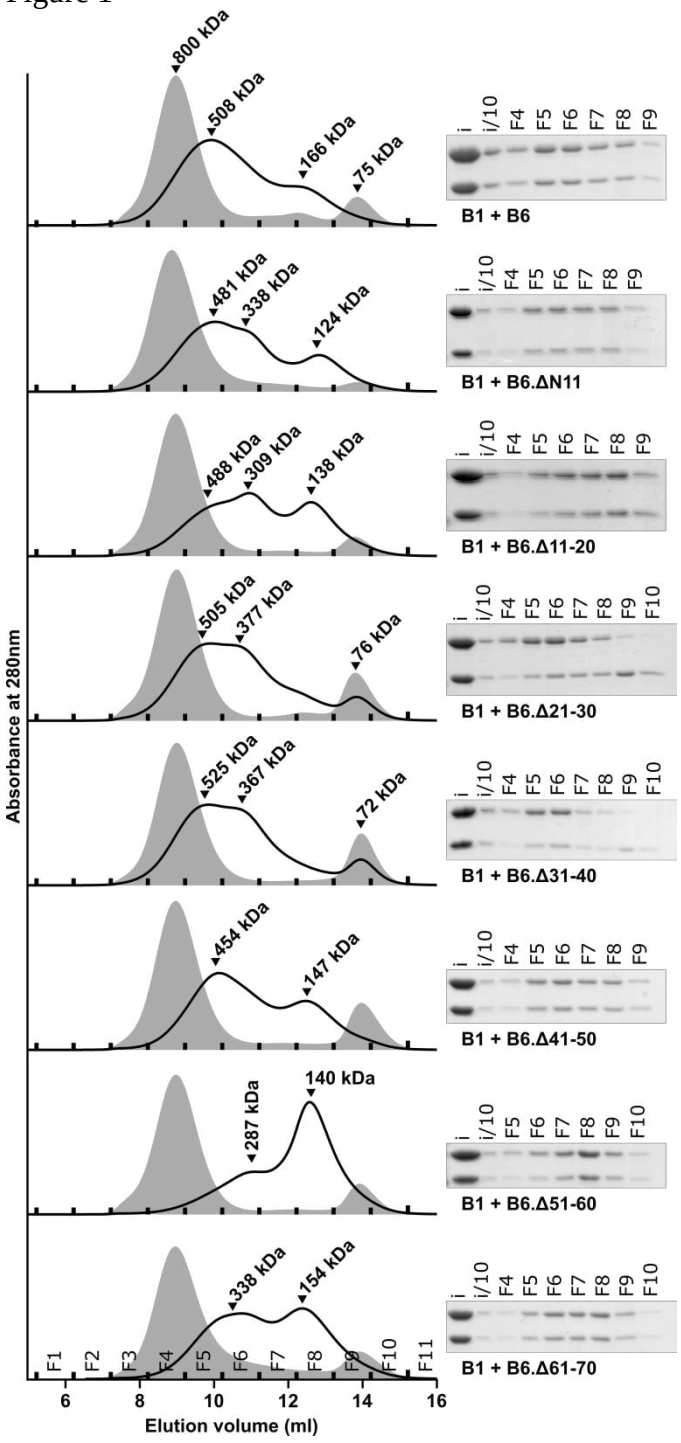
800 kDa
508 kDa
166 kDa
75 kDa
B1 + B6
481 kDa
338 kDa
124 kDa
B1 + B6.ΔN11
488 kDa
309 kDa
138 kDa
B1 + B6.Δ11-20
505 kDa
377 kDa
76 kDa
B1 + B6.Δ21-30
525 kDa
367 kDa
72 kDa
B1 + B6.Δ31-40
454 kDa
147 kDa
B1 + B6.Δ41-50
287 kDa
140 kDa
B1 + B6.Δ51-60
338 kDa
154 kDa
B1 + B6.Δ61-70
i
i/10
F1
F2
F3
F4
F5
F6
F7
F8
F9
F10
F11
Absorbance at 280nm
6
8
10
12
14
16
Elution volume (ml)

Figure 2

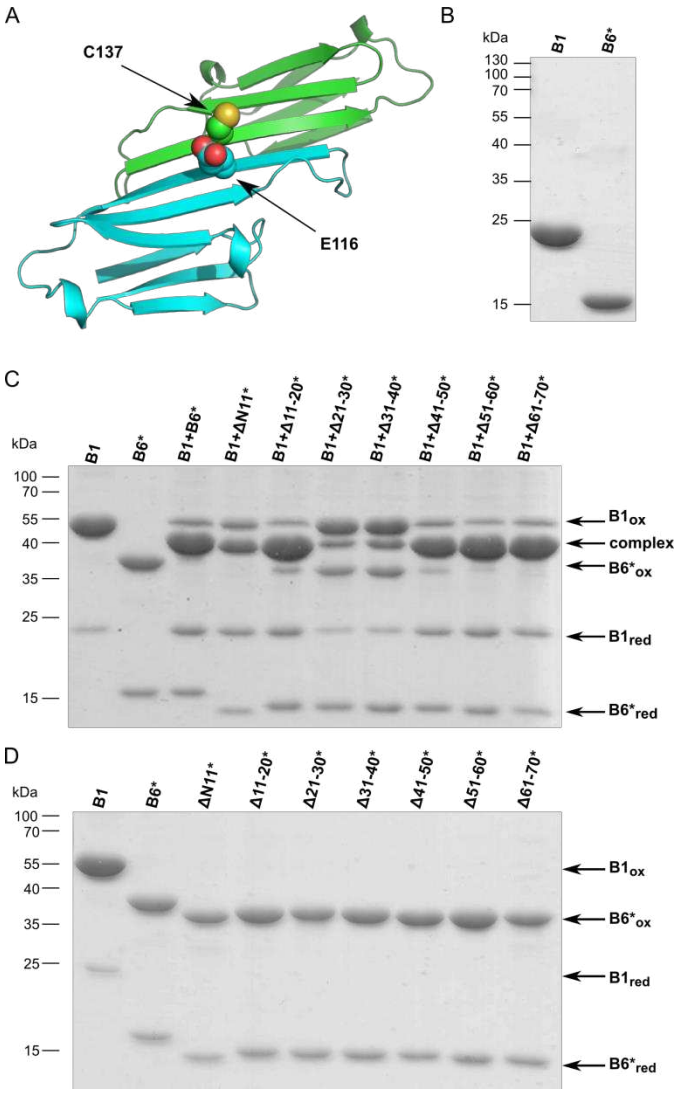
A
C137
E116
B
kDa
B1
B6*
130
100
70
55
40
35
25
15
C
kDa
B1
B6*
B1+B6*
B1+ΔN11*
B1+Δ11-20*
B1+Δ21-30*
B1+Δ31-40*
B1+Δ41-50*
B1+Δ51-60*
B1+Δ61-70*
100
70
55
40
35
25
15
B1ox
complex
B6*ox
B1red
B6*red
D
kDa
B1
B6*
ΔN11*
Δ11-20*
Δ21-30*
Δ31-40*
Δ41-50*
Δ51-60*
Δ61-70*
100
70
55
40
35
25
15
B1ox
B6*ox
B1red
B6*red

Figure 3

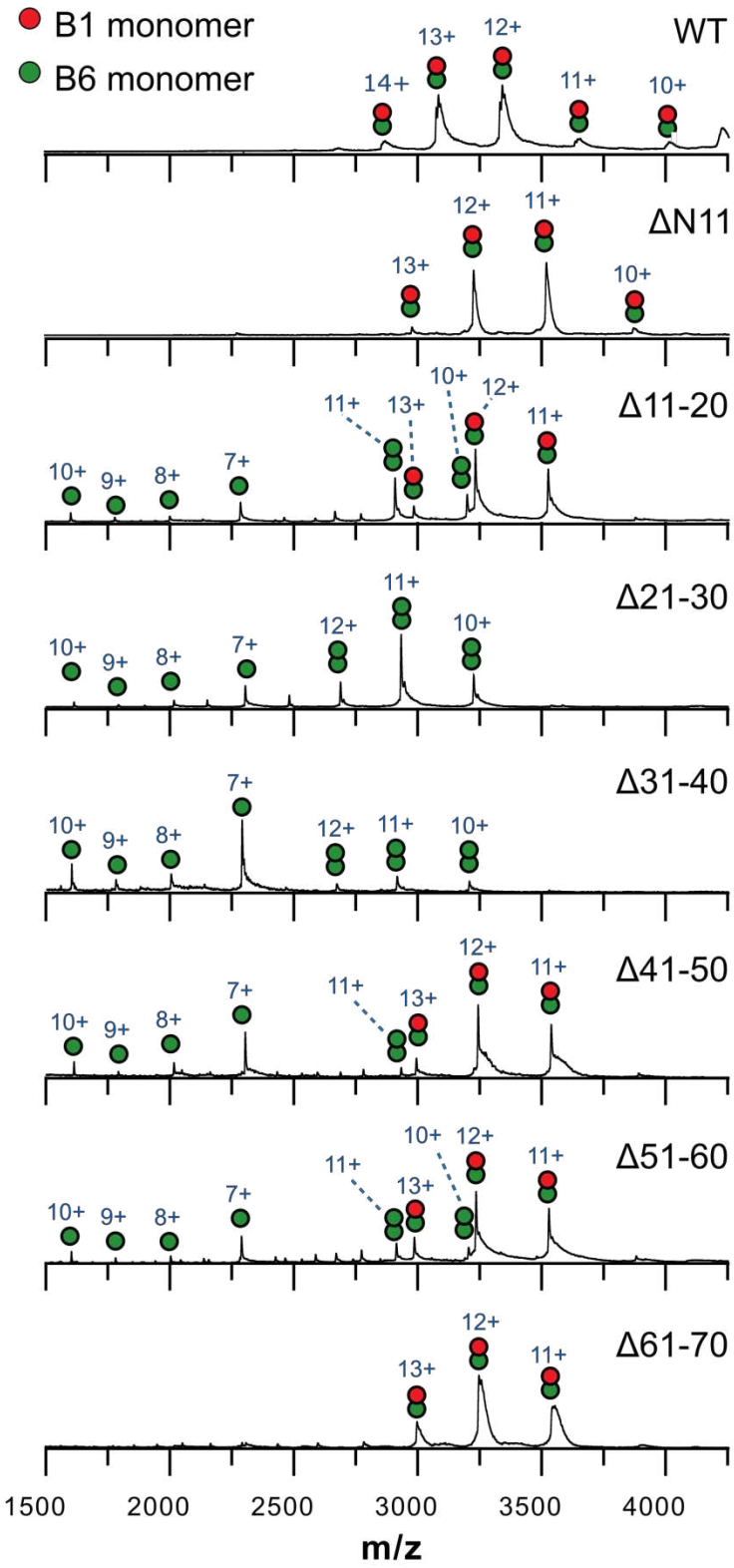
B1 monomer
B6 monomer
WT
14+
13+
12+
11+
10+
ΔN11
12+
11+
13+
10+
Δ11-20
11+
13+
10+
12+
11+
10+
9+
8+
7+
Δ21-30
11+
12+
10+
10+
9+
8+
7+
Δ31-40
7+
10+
9+
8+
12+
11+
10+
Δ41-50
12+
11+
11+
13+
7+
10+
9+
8+
Δ51-60
10+
12+
11+
11+
13+
7+
10+
9+
8+
Δ61-70
12+
11+
13+
1500
2000
2500
3000
3500
4000
m/z

Figure 4

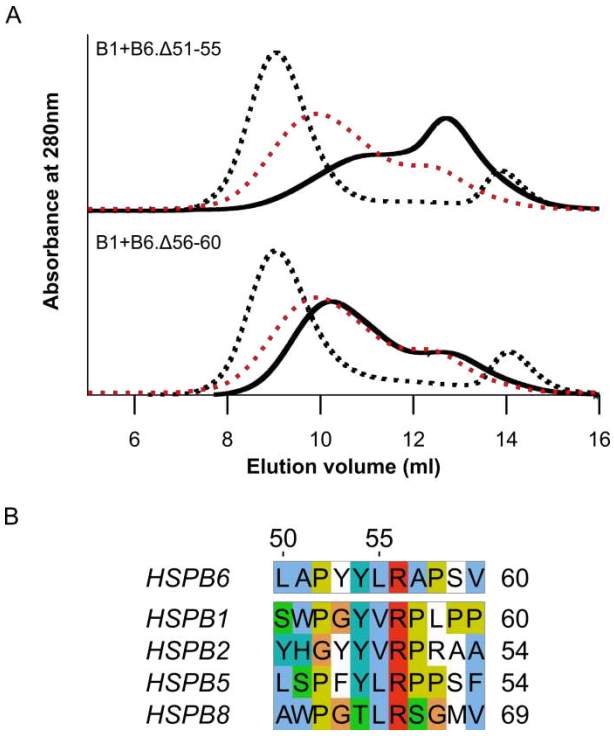
A
B1+B6.Δ51-55
B1+B6.Δ56-60
Absorbance at 280nm
6
8
10
12
14
16
Elution volume (ml)
B
50
55
HSPB6 LAPYYLRAPSV 60
HSPB1 SWPGYVRPLPP 60
HSPB2 YHGYYVRPRAA 54
HSPB5 LSPFYLRPPSF 54
HSPB8 AWPGTLRSGMV 69

Figure 5

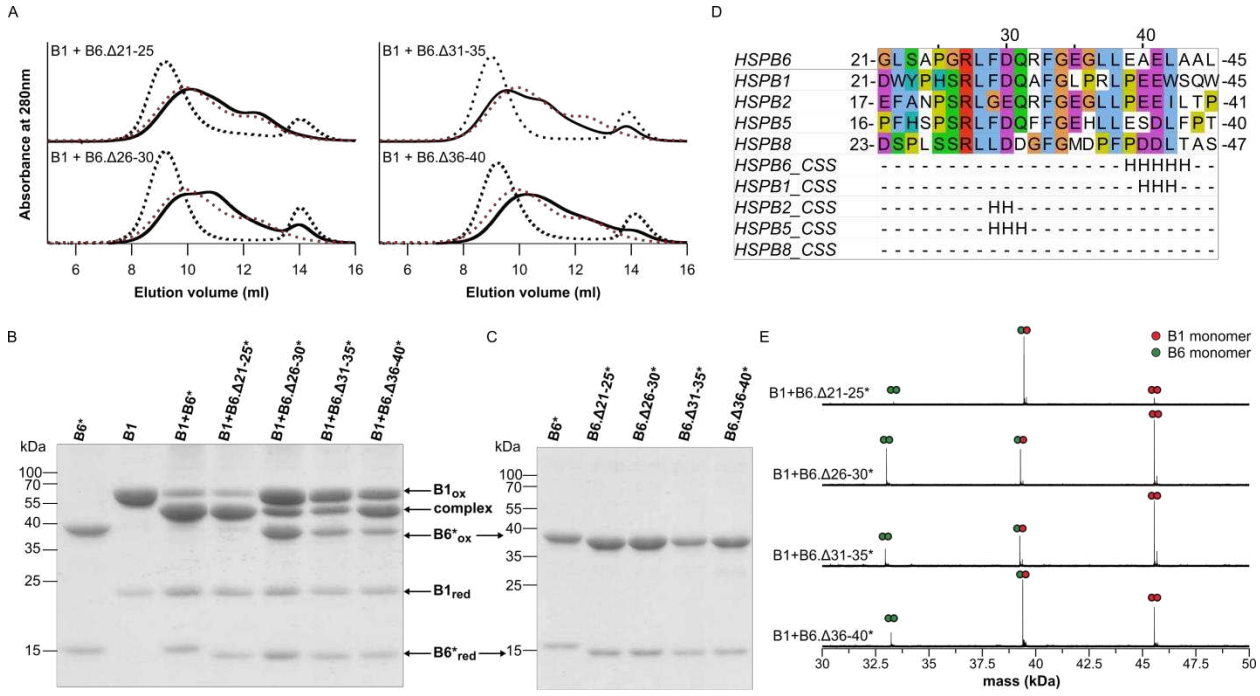
A
B1 + B6.Δ21-25
B1 + B6.Δ31-35
B1 + B6.Δ26-30
B1 + B6.Δ36-40
Absorbance at 280nm
Elution volume (ml)
Elution volume (ml)
D
30
40
HSPB6 21-GLSAPGRLFDQRFGEGLLEAELAAL-45
HSPB1 21-DWYPHSRLFDQAFGLPRLPEEWSQW-45
HSPB2 17-EFANPSRLGEQRFGEGLLPEEILTP-41
HSPB5 16-PFHSPSRLFDQFFGEHLLESDLFPT-40
HSPB8 23-DSPLSSRLLDDGFGMDPFPDDLTAS-47
HSPB6_CSS ----------HHHHH--
HSPB1_CSS ----------HHH---
HSPB2_CSS --------HH----------
HSPB5_CSS --------HHH---------
HSPB8_CSS ----------
B
kDa
B6*
B1
B1+B6*
B1+B6.Δ21-25*
B1+B6.Δ26-30*
B1+B6.Δ31-35*
B1+B6.Δ36-40*
B1ox
complex
B6*ox
B1red
B6*red
C
kDa
B6*
B6.Δ21-25*
B6.Δ26-30*
B6.Δ31-35*
B6.Δ36-40*
E
B1 monomer
B6 monomer
B1+B6.Δ21-25*
B1+B6.Δ26-30*
B1+B6.Δ31-35*
B1+B6.Δ36-40*
mass (kDa)

Figure 6

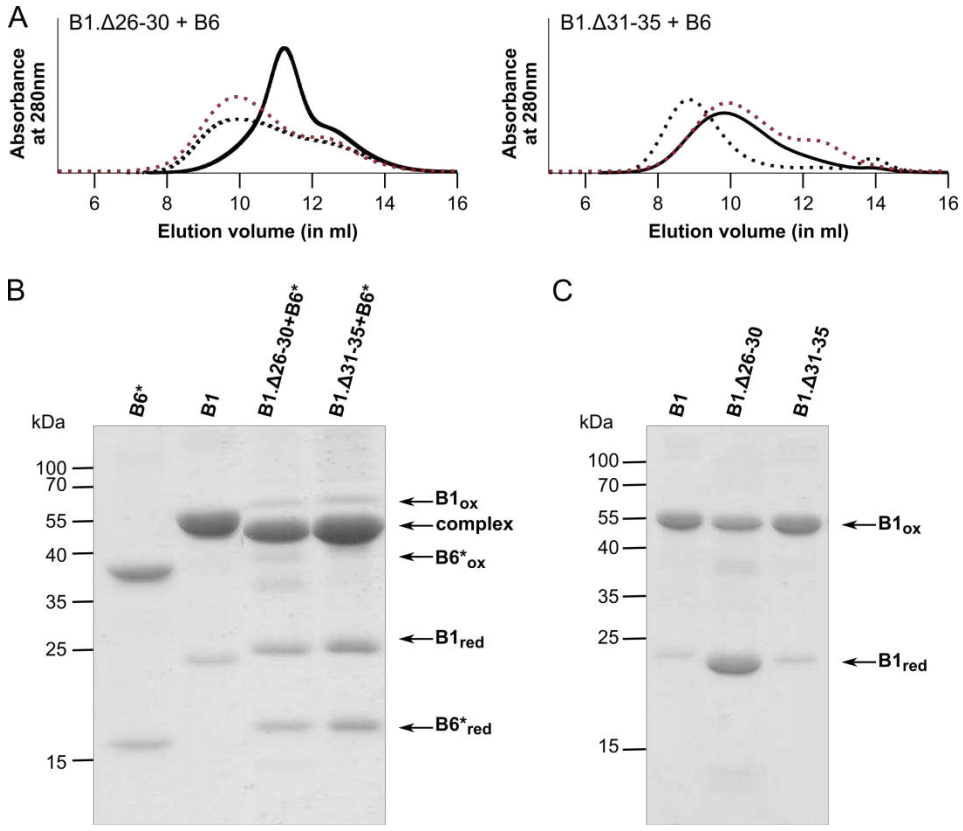
A
B1.Δ26-30 + B6
Absorbance at 280nm
6
8
10
12
14
16
Elution volume (in ml)
B1.Δ31-35 + B6
Absorbance at 280nm
6
8
10
12
14
16
Elution volume (in ml)
B
B6*
B1
B1.Δ26-30+B6*
B1.Δ31-35+B6*
kDa
100
70
55
40
35
25
15
B1ox
complex
B6*ox
B1red
B6*red
C
B1
B1.Δ26-30
B1.Δ31-35
kDa
100
70
55
40
35
25
15
B1ox
B1red

Figure 7

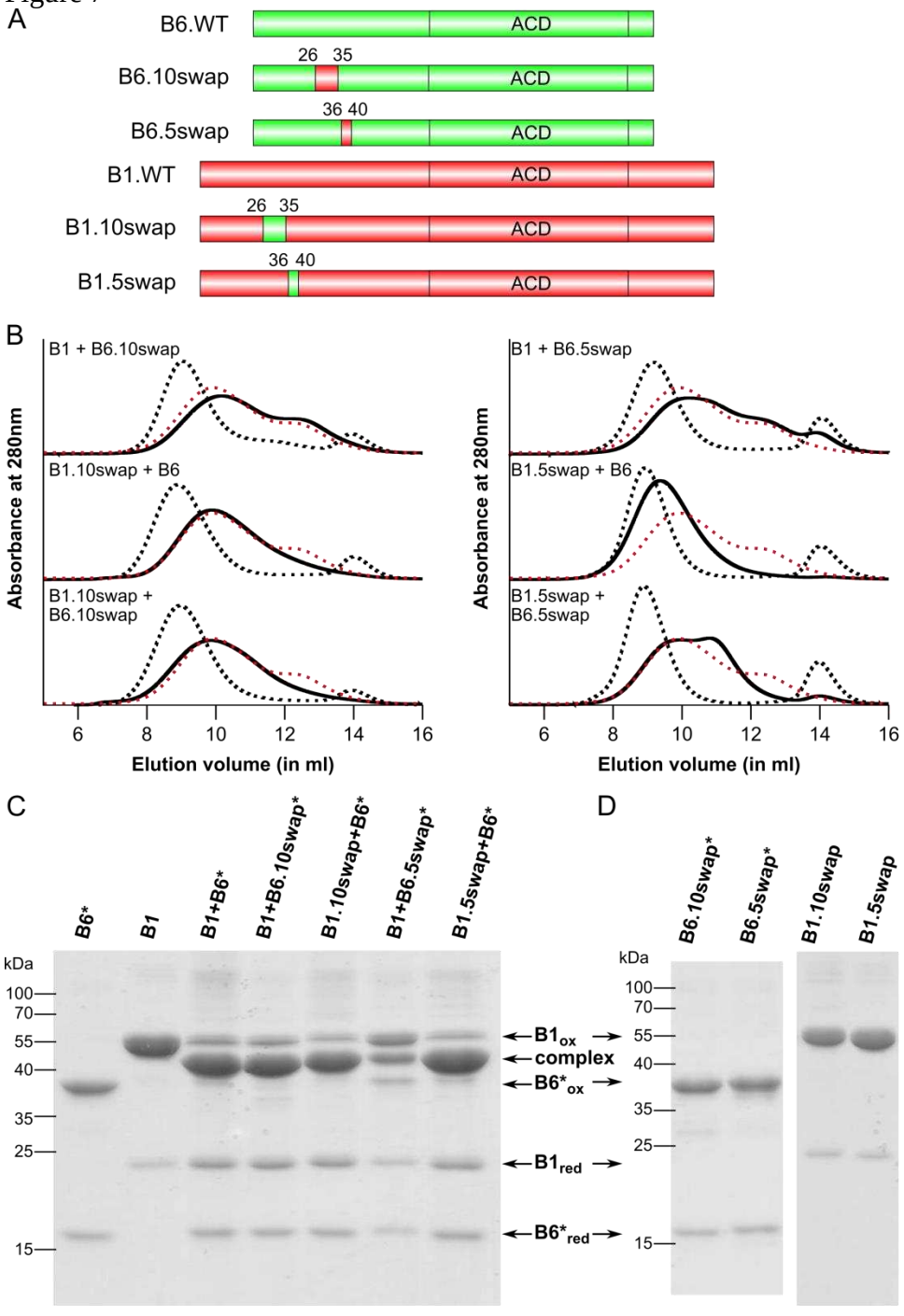
A
B6.WT
ACD
26 35
B6.10swap
36 40
B6.5swap
B1.WT
B1.10swap
B1.5swap
B
B1 + B6.10swap
B1.10swap + B6
B1.10swap + B6.10swap
B1 + B6.5swap
B1.5swap + B6
B1.5swap + B6.5swap
Absorbance at 280nm
Elution volume (in ml)
C
B6*
B1
B1+B6*
B1+B6.10swap*
B1.10swap+B6*
B1+B6.5swap*
B1.5swap+B6*
kDa
100
70
55
40
35
25
15
B1ox
complex
B6*ox
B1red
B6*red
D
B6.10swap*
B6.5swap*
B1.10swap
B1.5swap

Figure 8

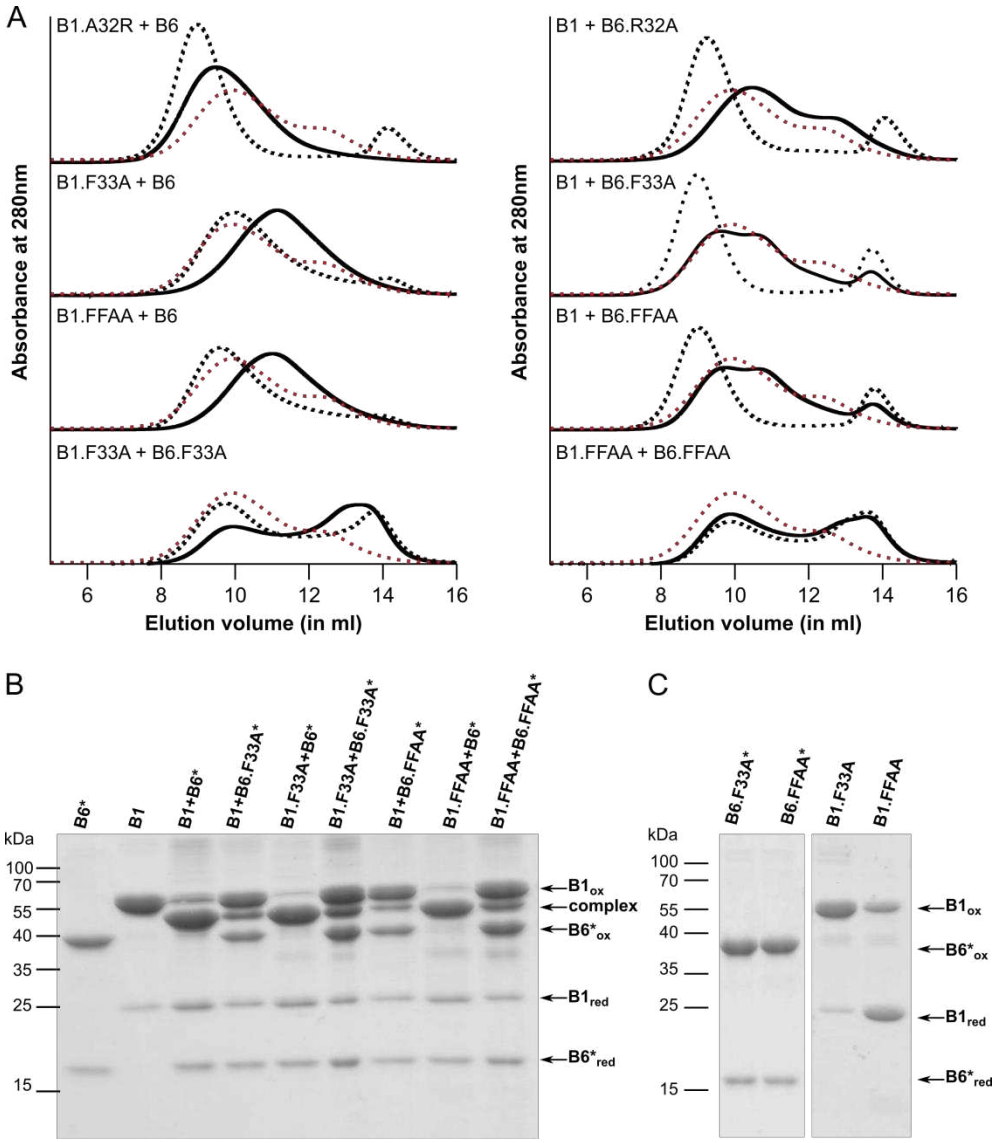
A
B1.A32R + B6
B1.F33A + B6
B1.FFAA + B6
B1.F33A + B6.F33A
B1 + B6.R32A
B1 + B6.F33A
B1 + B6.FFAA
B1.FFAA + B6.FFAA
Absorbance at 280nm
Elution volume (in ml)
B
C
B6*
B1
B1+B6*
B1+B6.F33A*
B1.F33A+B6*
B1.F33A+B6.F33A*
B1+B6.FFAA*
B1.FFAA+B6*
B1.FFAA+B6.FFAA*
B6.F33A*
B6.FFAA*
B1.F33A
B1.FFAA
kDa
100
70
55
40
35
25
15
B1ox
complex
B6*ox
B1red
B6*red

Figure 9

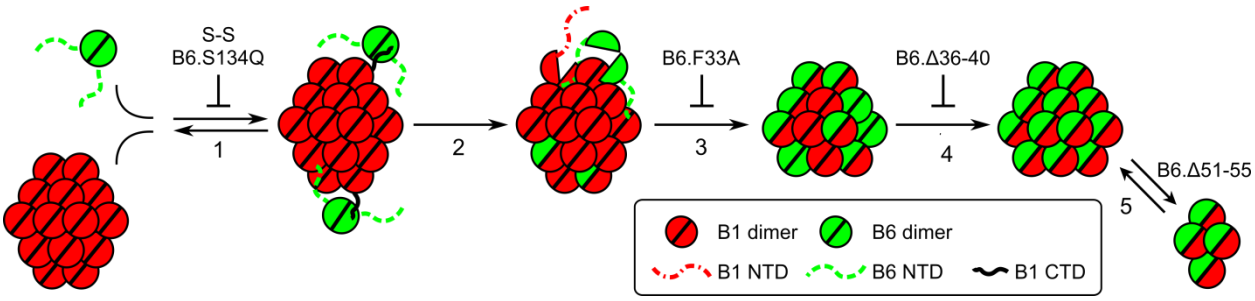
S-S
B6.S134Q
1
2
B6.F33A
3
B6.Δ36-40
4
5
B6.Δ51-55
B1 dimer
B6 dimer
B1 NTD
B6 NTD
B1 CTD